Review

Retrofitting of Steel Structures with CFRP: Literature Review and Research Needs

Mohamadreza Delzendeh Moghadam, Abbas Fathi and Omar Chaallal *

Department of Construction Engineering, École de Technologie Supérieure, University of Quebec, Montreal, QC H3C 1K3, Canada; mohamadreza.delzendeh-moghadam.1@ens.etsmtl.ca (M.D.M.); abbas.fathi.1@ens.etsmtl.ca (A.F.)

* Correspondence: omar.chaallal@etsmtl.ca

Abstract: The application of the externally bonded (EB) carbon fiber-reinforced polymer (CFRP) technique for retrofitting steel elements offers significant advantages over the conventional method. The high strength-to-weight ratio and corrosion resistance of CFRP materials have made them a viable alternative for retrofitting steel structures. This paper covers a wide range of aspects discussed in the research investigations to date on CFRP bonded steel elements and provides a critical review of the topic under both static and fatigue loading conditions. In the end, research needs and recommendations are presented in this respect.

Keywords: steel structures; retrofitting technique; carbon fiber-reinforced polymer (CFRP); bond–slip relationship; static loading; fatigue loading; finite element analysis; research progress

1. Introduction

Steel structures around the world are susceptible to deterioration over their service life period. This deterioration can reduce the potential strength and stiffness of the steel members due to cracks and corrosion induced by fatigue loading and extreme weather conditions, respectively. Additionally, defects may arise during the design and construction phases. The conventional approach for retrofitting steel structures is by using steel plates that are attached to the structure by weld or bolt [1]. However, this approach presents disadvantages, including the residual stress imposed by welding, which can lead to new damage to the structure [2,3]. Furthermore, the steel plates are susceptible to corrosion and their heavy weight poses challenges during installation [4,5]. Alternatively, the application of externally bonded carbon fiber-reinforced polymer (CFRP) can offer a durable solution to address these challenges [6,7]. The high strength-to-weight ratio and corrosion resistance of CFRP materials have an important role in their selection for retrofitting steel components [8–10].

In recent years, the application of advanced composite materials has been gaining acceptance in retrofitting civil infrastructures. Among these types of materials, CFRP and graphite fiber-reinforced polymer (GFRP) are well established [11]. However, CFRP exhibits superiority over GFRP due to its higher strength. Studies show that CFRP retrofitting systems can effectively enhance the flexural capacity of steel members and prolong their fatigue life [4,12–32]. CFRPs are classified based on their elastic modulus into Low Modulus (LM), Normal Modulus (NM) or Intermediate Modulus (IM), High Modulus (HM), and Ultra-High Modulus (UHM). There is not a unanimous approach to characterize the elastic modulus range of each category. However, it can be expressed relative to the steel elastic modulus as presented in Table 1 [33].

Table 1. CFRP classification in terms of elastic modulus [33].

CFRP Type	CFRP Modulus	CFRP Modulus Relative to Steel
Low Modulus (LM)	<100 GPa	$E_{CFRP} < 0.5\ E_{steel}$
Normal Modulus (NM)	100–200 GPa	$0.5\ E_{steel} \leq ECFRP < E_{steel}$
High Modulus (HM)	200–400 GPa	$E_{steel} \leq ECFRP < 2\ E_{steel}$
Ultra-High Modulus (UHM)	$\geq$400 GPa	$E_{CFRP} \geq 2\ E_{steel}$

The significance of this review lies in its comprehensive and up-to-date examination of the current state of knowledge on steel elements retrofitted with CFRP. This paper integrates findings from multiple dimensions and examines key parameters affecting the performance of CFRP retrofitted components and the bond behavior between CFRP and steel interfaces, including adhesive types, surface preparation, bond length, etc. By synthesizing findings from various investigations, this review aims to guide future research efforts and enhance the application of CFRP in retrofitting steel structures.

This paper is presented in the following sections: (i) a review of studies on the bond behavior between CFRP and steel; (ii) research findings regarding the flexural behavior of the retrofitted steel beams; and (iii) a review of numerical simulations of CFRP/steel retrofitted elements and their bond behavior. Finally, gaps in previous research are identified, and suggestions for further investigations are provided.

2. Bond Behavior between CFRP and Steel

The bond between CFRP and steel plays a major role in the performance of steel components retrofitted with CFRP. The role of the adhesive layer is to carry the tensile forces of the steel substrates and transfer them to the CFRP composites. A comparison between the CFRP/steel and CFRP/concrete bonded interfaces reveals the main contrast in terms of the bond behavior. Indeed, adhesives in the CFRP/steel joints are regarded as the weakest link, whereas the bond behavior of the CFRP/concrete shows that concrete acts as the weakest link [34]. Therefore, to achieve the maximum capacity of the CFRP retrofitting system that follows up with the CFRP rupture, the selection of the most effective adhesives is crucial [35]. Furthermore, many other parameters have been found influential on the bond behavior of the retrofitted elements. These parameters include the CFRP elastic modulus, CFRP bond length, CFRP configuration, adhesive type, adhesive thickness, anchorage system, and surface preparation of the steel substrate. It should be noted that temperature is also considered as one of these influential parameters. There are some comprehensive literature reviews that focus on the thermal and environmental effects [36,37].

2.1. Bond Test Configuration and Failure Modes

To study the bond behavior between the CFRP and steel substrate, two test setups have been mainly adapted, as shown in Figure 1. In the single strap joint configuration (a), two steel plates are attached by CFRP only on one side, while in the double strap joints configuration (b), CFRPs are attached to both sides of steel plates. In both configurations, the loading is applied to the steel plates. It should be noted that in the single strap joint test setup, the adherends are subjected to bending during loading due to load eccentricity. This asymmetrical configuration can lead to rotation of the bond plane, resulting in significant peel stresses at the adhesive layer ends, which may cause premature adhesive failure and consequently lead to an underestimation of the capacity of the CFRP/steel joint [38]. In contrast, the double strap joint is symmetrical about the mid-plane of the specimen. Therefore, given the adherends, the amount of peel stress due to bond rotation is considerably less than a single strap joint configuration [38]. Possible failure modes of the CFRP/steel joints under tensile loading include the following [5]: (a) adhesion failure at CFRP/adhesive interface; (b) adhesive layer failure; (c) adhesion failure at steel/adhesive interface; (d) CFRP delamination; (e) CFRP rupture; (f) steel yielding. Figure 2 presents a schematic view of these failure modes.
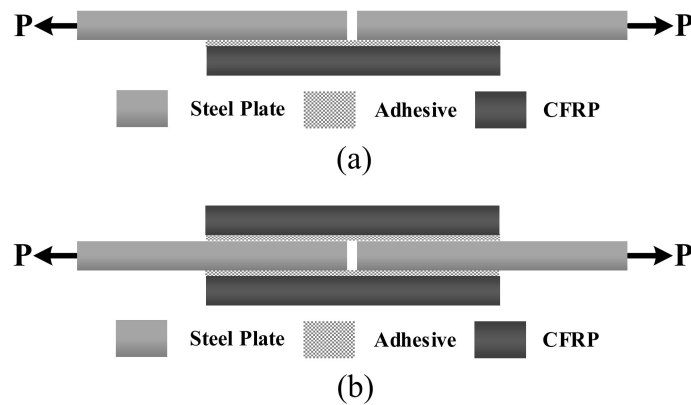
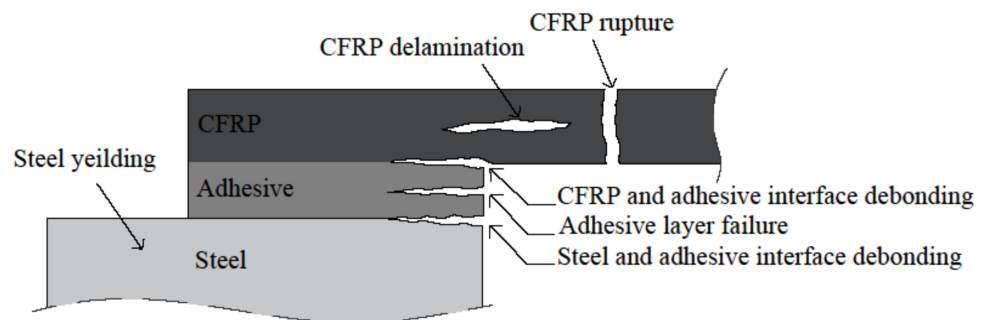**Figure 1.** Schematic view of the (**a**) single strap joint; (**b**) double strap joint test setups.

Figure 2. Possible failure modes of CFRP/steel joints under tensile loading [5].

Table 2 presents details of the previous studies on the bond behavior of CFRP/steel joints. It should be noted that in some research studies, the applied CFRP was claimed to be UHM. However, based on the classification presented in Table 1, they should be considered HM or NM CFRP. The elastic modulus of the applied CFRPs in these studies varied from 270 GPa to 640 GPa. However, investigations involving UHM CFRP have not been adequately documented. Based on these studies, it can be inferred that using CFRP with a higher elastic modulus can lead to an improvement in the load-carrying capacity of CFRP/steel joints [39]. Moreover, it has been found that the failure mode is altered as the elastic modulus and type of CFRP change [40,41]. Nevertheless, the influence of fatigue loading on bond behavior was reported to be insignificant, as only a limited bond region adjacent to the joint, known as the fatigue damage zone, was prone to fatigue damage [19]. It was also found that the failure mode changed as the temperature increased [42]. The dominated failure mode at elevated temperatures is cohesion failure within the adhesive layer [43]. In addition, the debonding loads of the CFRP/steel joints are notably decreased at both low and high service temperatures [44].

2.2. Adhesive

The mechanical properties of adhesive have a notable effect on the bond behavior of steel members retrofitted with CFRP [45–48]. As the adhesive is the weakest link in the CFRP and steel joint, selecting a proper adhesive can ensure the maximum capacity of the retrofitting system. In most research studies, commercial adhesives are utilized for retrofitting structures [34,49,50]. Figure 3 shows the stress–strain curves for these adhesives. It should be noted that the mechanical properties of the adhesive may decrease with increasing temperature [43]. Commercial adhesives have been found to possess insufficient strength, often resulting in brittle failure. Consequently, research efforts have been directed towards enhancing adhesive performance, particularly in terms of mechanical properties [45,51–55]. Utilizing enhanced adhesive can change the failure mode of the CFRP/steel joints [56,57].
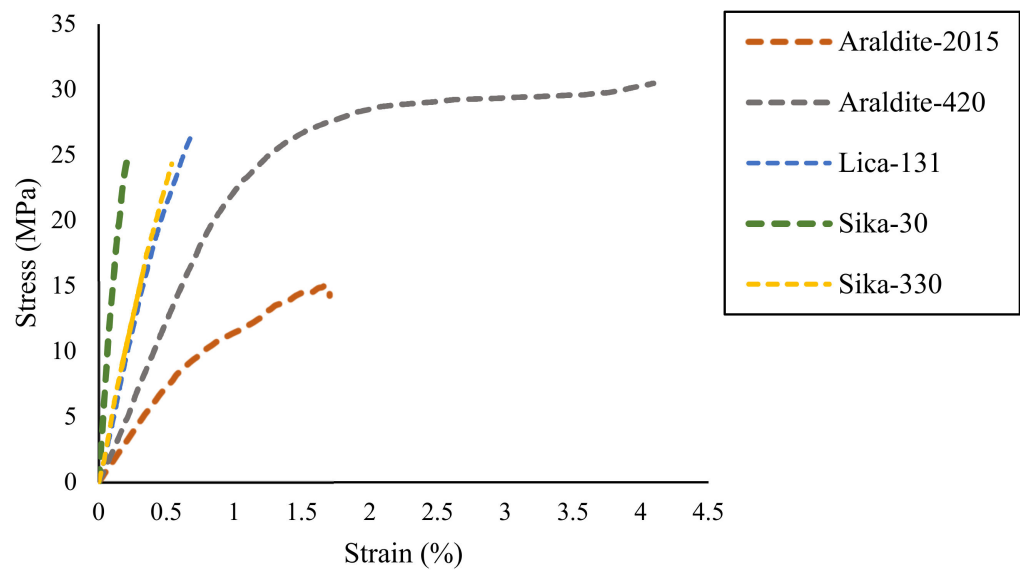
Figure 3. Tensile stress–strain curve of commercial adhesives used in bonding CFRP to steel substrate [45,49].

Among the commercial adhesives, Sikadur and Araldite have been commonly utilized. It was shown that specimens with Araldite 2015 adhesive exhibited a much higher interfacial fracture energy compared to the specimens with Sikadur 30 adhesive [49]. Indeed, specimens retrofitted with nonlinear adhesives having higher strain capacity but lower elastic modulus exhibit higher interfacial fracture energy and thereby a higher bond strength compared to the ones with linear adhesives having similar or even higher elastic modulus [34,58]. The type of adhesive can also significantly influence the bond–slip relationship. Bond–slip can be estimated as a triangular shape for linear adhesive and a trapezoidal shape for nonlinear adhesive [59]. The average effective bond length of specimens bonded with nonlinear adhesive was also found to be greater than that of specimens with linear adhesive, which could be attributable to the higher ductile behavior of nonlinear adhesive compared to the linear one [60]. It is also found that the effective bond length, interfacial fracture energy, and ultimate load increase with the increase in adhesive thickness [49,61]. In addition, increasing the adhesive thickness can change the failure mode from cohesive failure to CFRP delamination [34,62,63]. However, specimens with lower adhesive thickness exhibited better performance in terms of the average peel stresses and failure load [64]. It is worth mentioning that assessing the effect of adhesive thickness on the failure mode is difficult due to the non-uniform thickness of the bond-line [65]. It is suggested to increase the adhesive thickness up to 2 mm to avoid cohesive failure [63,66]. Non-cohesive failure in the bond test has been reported in the literature [34,47,60,67–69]. Increasing the adhesive thickness to 3 mm may result in lower bond strength compared to a thickness of 2 mm [34]. Consequently, it can be concluded that the adhesive's mechanical properties and thickness are the key factors in the bond behavior of CFRP retrofitted steel components [49,55]. Furthermore, the adhesive layer, regardless of the type of adhesive, can help prevent potential galvanic corrosion if the bond quality is strictly controlled [70]. Furthermore, investigations on the impact of bond-line defects on the bond behavior of CFRP steel joints suggest that the size of the defect plays a more significant role in determining the failure mode than the number of defects [71].

Table 2. Experimental details of studies regarding the bond behavior of CFRP/steel joints. Note: (a) adhesive thickness, (b) adhesive type, (c) adhesive elastic modulus, (d) steel stiffeners, (e) CFRP configurations, (f) CFRP thickness, (g) CFRP to steel width ratio, (h) CFRP bond length, (i) CFRP axial rigidity, (j) loading amplitude.

Ref.	f_y (MPa)	E_s (GPa)	f_a (MPa)	E_a (GPa)	t_a (mm)	f_p (MPa)	E_p (GPa)	t_p (mm)	Type of CFRP	Test Set-Up	Steel Plate (mm) ($L_s \times w_s \times t_s$)	a	b	c	d	e	f	g	h	i	j
[64]	375	205	14.8 43 32	6.8–7.3 2.1 3.5	0.1 0.5 1	2109.3 1120.8	135.3 270.1	1.2	NM HM	S * D *	225 × 25 × 1.5 225 × 25 × 3 225 × 25 × 6	✔	✔	✔		✔					✔
[63]	—	—	22.53 20.48 13.89	4.01 10.79 5.43	1 2 3 4	—	165	1.2	NM	S	305 × 118 × 12	✔	✔	✔							
[72]	—	—	37.1	3	1	—	338 460	4 8	HM UHM	D	$L_S = 200, 400$							✔	✔		
[73]	317.8	—	24.8 30	4.5 3.8	0.8 1	>2800	197	1.4	NM	D	460 × 60 × 6 600 × 60 × 6 1200 × 60 × 60		✔			✔					
[35]	—	200	76	3.1	-	2448 1190	640 340	0.19 1.42	UHM HM	D	128.2 × 25.4 × 3.3 258.3 × 25.4 × 3.3		✔			✔	✔		✔		
[39]	409	200	34.6	3	0.6–0.7	2979 1923	187 514	1.2	NM UHM	D	250 × 50 × 4.8 300 × 50 × 4.8 610 × 50 × 4.8								✔		
[60]	300	200	28.6 24	1.9 9.2	var	1500	460	1.45	UHM	D	300 × 50 × 30		✔							✔	
[34]	—	200	22.34 31.28 14.73 21.46	11.25 4.82 1.75 1.83	0.5 2 3	—	150 235 340	1.2 1.4	NM MM HM	S	$L_S = 450$ $t_S = 30$	✔	✔							✔	
[74]	359	200	32	1.9	-	2300	256	-	HM	D	180 × 50 × 5										✔
[19]	487	200.6	28.6	1.90	0.66	1607	478.73	1.45	UHM	D	300 × 50 × 10										✔
[75]	300	—	33.16	11.3	1	1970	185	1.44	NM	S	** 100 × 100 $L_S = 250$ $t_S = 5$										
[9]	235	210	35	—	var	—	460	-	UHM	D	450 × 60 × 15 450 × 60 × 10	✔									
[76]	410	—	34.6	3.01	-	1200 2800	450 165	1.2	UHM NM	D	610 × 50 × 5 610 × 50 × 4.8 610 × 50 × 9.5							✔		✔	
[49]	414	198	27.6 15.1	12.2–1.75	var	2760	164	1.4	NM	S	$t_S = 20$	✔	✔								
[18]	235	-	26–31	11.2	1–2	3100	170	1.2	NM	D	$w_S = 75$ $t_S = 12$								✔		
[77]	400	210	21.76	8.4	-	1820 1840	180.5 163.3	1.46 1.26	NM	D	$w_S = 55$ $t_S = 5$							✔			

* S = single strap joints/D = double strap joints; ** square steel tubes.

2.3. Surface Preparation

Surface preparation is one of the most crucial parameters of the bond behavior of the CFRP retrofitted elements. The bond capacity can be determined by the cohesion strength of the adhesive as well as the adhesion strength of the interface between the adhesive and the substrate [78]. Adhesion failure can occur at the CFRP/adhesive or the steel/adhesive interface. However, debonding at the steel/adhesive interface is more likely to occur [6,79]. Therefore, the preparation of the steel substrate has received more attention. The adhesion is mainly provided by mechanical interlocking and chemical bonding between the adhesive and the adherend [80]. It is debatable regarding the agent that is responsible for strong bonds. However, it seems that chemical bonding is more important than mechanical bonding [6]. To improve the mechanical bonding, the steel substrate is roughened before the CFRP bonding process. However, applying an improper roughening technique may cause tiny crevices in which the trapped air bubbles or solvent can induce failure in a rigid adhesive by increasing the stress concentrations [81]. It can also reduce the contact between the adhesive and the adherent, which is so-called wetting [82]. Indeed, increasing the contact surface area leads to enhanced wetting and more extensive chemical bonding [83]. The most commonly used mechanical treatments are grit blasting, needle scaler, and sandpaper. In these abrasive techniques, the surface geometry of the substrate is modified and the oxide layer is removed. It is generally accepted that using the grit blasting method is effective [2,6,78]. It also can lead to modifying the surface chemical composition by removing the contaminants such as oil and grease. However, it can introduce grit residues or other contaminants onto the steel substrate [84]. Furthermore, the grit type should be carefully chosen to ensure chemical compatibility with the applied adhesive [78]. Improper surface preparation can lead to premature failure, thereby hindering the achievement of the full capacity of the CFRP retrofitting technique.

2.4. Bond Length

Research findings show that the bond strength, as well as the failure modes of CFRP bonded steel elements, can be affected by the bond length [85]. The bond strength of the CFRP/steel interface tends to increase at greater bond lengths. The strain level experienced by the applied adhesive was seen to drop significantly when a longer bond length was used [85]. Therefore, it is more likely for specimens with shorter bond lengths to undergo debonding failure, whereas steel components retrofitted with greater CFRP bond lengths are more likely to fail due to CFRP rupture. However, increasing the bond length from a certain threshold, the so-called effective bond length, does not yield a further increase in the bond strength [59,86–90]. Moreover, increasing either the CFRP elastic modulus or CFRP thickness results in an increase in CFRP/steel bond strength, although applying CFRP with higher axial stiffness seems to require a greater bond length [90,91]. Furthermore, the type of adhesive has a significant effect on the effective bond length [92]. Applying the nonlinear adhesive can increase the bond strength and the effective bond length compared to the linear adhesive as a result of its ductile behavior and larger elongation at break [60]. It was also found that the rate of impact loading has a trivial effect on the effective bond length; however, it has a notable effect on the bond strength and failure modes [46,90,93–95]. Although the effect of bond length on the stiffness of the retrofitted elements is negligible, it can increase the load-carrying capacity of the components [12]. The proposed formulas to calculate the effective bond length are provided in Table 3. As observed, the ultimate load is not influenced by the adhesive thickness. This issue is also the same for calculating the ultimate load in CFRP/concrete joints [96].

Table 3. Bond strength and effective bond length for CFRP/steel interface.

Ref.	Effective Bond Length	Maximum Shear Stress	Ultimate Load	Remarks
[63]	$\frac{\pi}{2\sqrt{\tau_f/E_p t_p \delta_f}}$	$0.8f_a$	$b_p\sqrt{2G_f E_p t_p}$	-
[97]	$2.77\sqrt{\frac{\beta}{\beta+1}} \times \frac{\sqrt{2G_f E_p t_p}}{\tau_f}$	$\sqrt{\frac{G_a G_f}{2.72 t_a}}$	$N\sqrt{\frac{\beta+1}{\beta}} \times b_p\sqrt{2G_f E_p t_p}$	$\beta = \frac{b_s t_s E_s}{2b_p t_p E_p}$
[98]	$3.5\sqrt{\frac{E_p t_p t_a}{G_a}}$	$0.8f_a$	$b_p\sqrt{2G_f E_p t_p}$	-
[99]	$a_d + b_e + \frac{1}{\lambda_1}\ln\left(\frac{1+C}{1-C}\right)$	$0.9f_a$	$b_p\sqrt{2G_f E_p t_p}$	$a_d = \frac{1}{\lambda_1}\left[\sqrt{\left(2\frac{\delta_2}{\delta_1}-1\right)}-1\right]$ $b_e = \frac{1}{\lambda_2}arcsin\left[\frac{\lambda_2\lambda}{0.97\delta_1\lambda_1^2}\left(\delta_f-\delta_2\right)\right]$ $C = \frac{\lambda_2}{\lambda_1\delta_1}\left(\delta_f-\delta_2\right)\cot(\lambda_2 b_e) - \lambda_1 a_d$ $\lambda^2 = \frac{\tau_f}{2G_f}\left(\frac{1}{E_p t_p} + \frac{b_p}{E_s t_s b_s}\right)$ $\lambda_1^2 = \frac{2G_f}{\tau_f \delta_1}\lambda^2$ $\lambda_2^2 = \frac{2G_f}{\tau_f\left(\delta_f-\delta_2\right)}\lambda^2$
[86]	$\delta_1\sqrt{\frac{2E_p t_p}{G_f(1+2\beta)}}$	-	$b_p\sqrt{2G_f E_p t_p(1+2\alpha)}$	$\alpha = \frac{b_p E_p t_p}{b_s E_s t_s}$

2.5. Bond–Slip Models

The bond–slip model presents a formula that predicts the interfacial fracture energy based on the adhesive properties [59]. The effective bond length and bond strength can be achieved by the bond–slip relationship. This relationship can be experimentally determined from strain gauges along the bond length through bonded joint tests [62]. The bond–slip curve for linear adhesive is different from that of nonlinear adhesive. Linear adhesives have an approximately bi-linear shape. However, nonlinear adhesives exhibit an approximately trapezoidal shape, as presented in Table 4. As for the CFRP/concrete joints, the bond–slip curve always has a roughly bi-linear shape due to the brittle behavior of concrete [34]. Therefore, the bond–slip models for CFRP/steel joints are different and should be developed based on the adhesive behavior. A number of bond–slip models have been proposed for CFRP/steel bonded joints, as shown in Table 5.

Table 4. Type of bond–slip models.

Ref.	Type of Model	Bond–Slip Model	Bond–Slip Curves
[100]	Bi-linear	$\begin{cases} \tau = \tau_f \frac{\delta}{\delta_1} & \delta \leq \delta_1 \\ \tau = \tau_f \frac{\delta_f-\delta}{\delta_f-\delta_1} & \delta_1 < \delta \leq \delta_f \\ \tau = 0 & \delta > \delta_f \end{cases}$	
[101]	Simplified	$\begin{cases} \tau = \tau_f\sqrt{\frac{\delta}{\delta_1}} & \delta \leq \delta_1 \\ \tau = \tau_f\exp\left[-\alpha\left(\frac{\delta}{\delta_1}-1\right)\right] & \delta > \delta_1 \\ \alpha = \frac{3\tau_f\delta_1}{3G_f-2\tau_f\delta_1} \end{cases}$	

Table 4. *Cont.*

Ref.	Type of Model	Bond–Slip Model	Bond–Slip Curves
[98]	Tri-linear	$\begin{cases} \tau = \tau_f \frac{\delta}{\delta_1} & \delta \leq \delta_1 \\ \tau = \tau_f & \delta_1 < \delta \leq \delta_2 \\ \tau = \tau_f \frac{\delta_f - \delta}{\delta_f - \delta_2} & \delta_2 < \delta \leq \delta_f \\ \tau = 0 & \delta > \delta_f \end{cases}$	

The bond–slip models are categorized as bi-linear, tri-linear, and simplified models. Bi-linear and simplified models were proposed for FRP/concrete and FRP/steel interfaces. The parameters of the bond–slip models for FRP/concrete bonded joints are expressed based on the tensile strength of the concrete, as the concrete is commonly the weakest link of the joint [59]. However, for CFRP/steel joints, these parameters are defined based on the tensile strength of adhesive since the weakest link of the joint is usually adhesive. In addition, the tri-linear model was presented for only CFRP/steel interfaces and utilized for nonlinear adhesive. It should be noted that the area under the curve is representative of the interfacial fracture energy in these models [102,103].

Table 5. Bond–slip models proposed for CFRP/steel interface.

Ref.	Type of Model	τ_f	δ_1	δ_2	δ_f
[63]	Bi-linear	$0.8 f_a$	$0.8 \frac{t_a}{G_a} f_a$	N/A	$\frac{2G_f}{\tau_f}$
[67]	Bi-linear	f_a	$\frac{t_a}{10}$	N/A	$\begin{cases} \frac{t_a}{4} & if\ t_a = 0.1\text{–}0.5\ mm \\ 0.125 + \frac{t_a - 0.5}{10} & if\ t_a = 0.5\text{–}1\ mm \end{cases}$
[59]	Bi-linear	$0.9 f_a$	$0.3 \left(\frac{t_a}{G_a}\right)^{0.65} f_a$	N/A	$\frac{2G_f}{\tau_f}$
[59]	Simplified	$0.8 f_a$	$0.3 \left(\frac{t_a}{G_a}\right)^{0.65} f_a$	N/A	-
[98]	Tri-linear	$0.8 f_a$	$0.8 \frac{t_a}{G_a} f_a$	$\frac{\delta_f}{3}$	$\frac{3G_f}{2\tau_f} + \frac{3}{4}\delta_1$
[49]	Bi-linear	$0.9 f_a$	$2.61 \frac{t_a^{0.34}}{G_a} f_a$	N/A	$166.2 \frac{t_a^{0.4}}{E_a^{1.7}} f_a^{2.4}$
[49]	Tri-linear	$0.9 f_a$	$2.61 \frac{t_a^{0.34}}{G_a} f_a$	$55.4 \frac{t_a^{0.4} f_a^{2.4}}{E_a^{1.7}} + 0.85 \frac{t_a^{0.34} f_a}{G_a}$	$\frac{2}{3}\left(\frac{2G_f}{\tau_f} + \delta_1\right)$
[104]	Bi-linear	$0.544 \tau^{*1.21}$	$1.51 \frac{t_a^{0.378}}{G_a} \tau^{*1.21}$	N/A	$\frac{2G_f}{\tau_f}$

3. Flexural Retrofitting of Steel Beams

This section reviews the studies related to the flexural behavior of the steel structures retrofitted with CFRP. Various modes of failure in CFRP retrofitted beams were reported, as shown in Figure 4, such as (a) CFRP end-debonding and intermediate-debonding; (b) CFRP delamination or rupture; (c) bending failure in which yielding occurs in beam flanges and web; (d) local bucking, which occurs in compression flange or web; (e) lateral-torsional buckling [18]. To investigate CFRP retrofitting technique efficiency, the lateral and local buckling of steel beams should be controlled or eliminated [105]. Among the aforementioned failure modes, the debonding of the CFRP has been found as the dominant failure mode for the specimens retrofitted with NM CFRP [18,106–109]. CFRP end-debonding is the common failure mode for beams that are retrofitted in flexural yielding [18]. It should be noted that if a longer CFRP plate is applied, the failure mode could turn into a different failure mode, in particular, intermediate-debonding [109]. On the other hand, the CFRP rupture was reported as the common failure mode for HM and UHM CFRP [5,13]. This phenomenon occurs due to the lower rupture strain of CFRP featuring a higher elastic modulus and the reduced stresses of the adhesives at the ends [39]. However, strengthened steel beams using UHM CFRP strips showed debonding failure at strip panel finger joints due to high shear stresses [110]. The most studied parameters in existing research investigations of CFRP retrofitted structures in flexure include adhesive thickness, adhesive type, CFRP configurations, CFRP thickness, and CFRP bond length. Details of previous studies on the

flexural behavior of the CFRP-strengthened and rehabilitated steel beams are presented in Table 6.
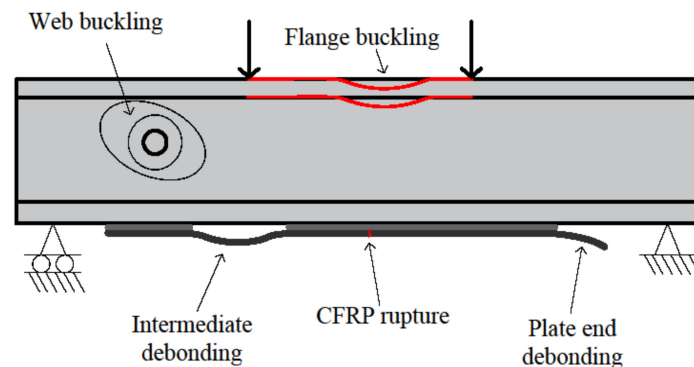

Figure 4. Some of the failure modes of steel beams strengthened with FRP plate [111].

Experimental observations on the effect of CFRP retrofitting systems on steel–concrete composite beams indicated a significant strength increase in specimens retrofitted with CFRP [13,112]. In these cases, concrete crushing and CFRP rupture were reported as the main failure modes. In addition, it was suggested to attach CFRP laminates to beam webs which can lead to a decrease in the interfacial shear stress of the adhesive between the bottom CFRP plate and the steel due to shifting the neutral axis to a lower level [112]. The application of small-diameter strands of CFRP was also found effective in flexural strengthening of steel bridge girder, especially for NM CFRP [113].

The flexural capacity of the steel beams can also be enhanced by using CFRP laminates with higher tensile strength or increased thickness [15]. Furthermore, the CFRP laminates with higher elastic modulus have a better performance in enhancing the ductility of the strengthened beams [112]. Failure analysis and structural behavior of CFRP-strengthened steel beams show that the load-carrying capacity with thicker and longer CFRP plates increases, though excessive thickness could cause premature debonding [114].

In order to prevent debonding failure and use the full capacity of the CFRP, mechanical anchorage systems have been utilized. It was shown that the mechanically fastened CFRP technique outperformed CFRP sheets in flexural strength and ductility [115]. Moreover, the application of the anchorage system to hybrid FRP also resulted in the same results [17]. Furthermore, in this case, prestressing CFRP increases the efficiency of the retrofitting method [116]. In addition, this technique can delay crack propagation and also results in an increase in the fatigue life of specimens [117].

A comparison between the performance of different FRP techniques as well as using steel plates for retrofitting reveal that HM CFRP is superior to the other rehabilitation methods in terms of fatigue behavior [118]. CFRP can significantly extend the fatigue life of the steel specimens and increase the average number of load cycles to failure [4]. Furthermore, CFRP materials can enhance the flexural fatigue behavior of the steel beams in terms of elastic stiffness, yield load, and nominal capacity [119]. The CFRP retrofitting method can also contribute to a reduction in fatigue crack growth in damaged steel beams [20]. In this regard, the elastic modulus of the CFRP is also found an important parameter in enhancing the fatigue life of specimens. Specimens retrofitted with higher elastic modulus outperform those retrofitted with CFRP with lower elastic modulus [120]. Furthermore, the stress intensity factor can be affected by the number of CFRP layers. It was shown that the stress intensity factor in specimens with a double CFRP configuration is significantly less than of the specimens strengthened with a single CFRP layer [24].

Table 6. Experimental flexural tests on CFRP retrofitted steel specimens.

Ref.	Loading Condition	Test Setup	L_{span} (mm)	Steel Cross Section (mm)	E_s (GPa)	f_y (MPa)	f_u (MPa)	CFRP Type	t_p (mm)	E_p (GPa)	f_p (MPa)	Adhesive Type	t_a (mm)	E_a (GPa)	f_a (MPa)	τ_a (MPa)
[112]	Static	F *	3048	** W8 × 15	-	363.4	496.4	NM HM	1.4	152 200	2482 >2482	-	-	-	68.9	-
[4]	Fatigue	F	1300	S127 × 4.5	194.4 (flange) 199.9 (web)	336.4 (flange) 330.9 (web)	-	NM	-	144	2137	-	-	-	-	-
[32]	Static	T *	2743.2	W12 × 14	-	-	-	HM	1.4	>200	>2300	-	-	-	-	-
[121]	Fatigue	F	-	W14 × 68	-	340	-	NM	-	157 114	2600 790	Sikadur 330 Sikadur 30 PLUS 25 DP-460 NS Tyfo TC	-	4.6 - - 1.8 -	41 25 17 35 47	-
[122]	Static Fatigue	F	1800	W100 × 17.5	200	-	-	HM	1.4	300	1800	Sikadur 30	-	2.75	-	-
[119]	Fatigue	F	-	W200 × 19	200	380	-	UHM	-	460	-	-	-	-	-	-
[13]	Static	F	6550	** W310 × 45	-	369–408	-	NM UHM	3.2 2.9 4	229 457	1224 1534	Spabond-345	-	-	-	-
[106]	Static	T	2500	HEA140	-	331	469	NM	1.4	197	>2800	Sikadur 30 Sikadur-330	-	4.5 3.8	24.8 30	24.8 -
[108]	Static	T and F	1200	127 × 76UB13	205	-	-	HM	3 6	212	-	Sikadur 30	1	8	29.7	-
[15]	Static	F	2000	HEA180	212	330	-	NM HM	1.4 1.8 2.4	200 330 165	3300 1500 3100	-	2	7 4.5	25 30	-
[120]	Fatigue	F	-	W310 × 74	200	350	450	NM HM	-	165 210	2520 2805	Sikadur-30	-	-	-	-
[39,110]	Static	F	2743	** W10 × 22 C7 × 9.8	200	407 414	510 531	UHM	1.2	514	1923	Spabond-345	2.5	3	34.6	-
[85]	Static	F	2000	I-section beam: $w_b = 100$ $h_b = 150$ $t_f = 10$ $t_w = 6.6$	-	250	370	NM	1.2	165	3100	Sikadur-30	1	11.2	24–31	14–19
[118]	Fatigue	F	-	H350 × 175	-	-	-	UHM NM SW-BFRP	-	436.4 145 108.3	1500 2500 1789	Sikadur-30	-	2.627	31.7	14.4
[115]	Static	F	2000	** UC203 × 203 × 46	200	318.75	459	LM	-	65.364	736.6	Sikadur-330	-	4.5	30	-

Table 6. *Cont.*

Ref.	Loading Condition	Test Setup	L_{span} (mm)	Steel Cross Section (mm)	E_s (GPa)	f_y (MPa)	f_u (MPa)	CFRP Type	t_p (mm)	E_p (GPa)	f_p (MPa)	Adhesive Type	t_a (mm)	E_a (GPa)	f_a (MPa)	τ_a (MPa)
[113]	Static/cyclic/fatigue	F	3350	W8 × 13	-	-	-	NM HM	-	134.6 226.3	2288 2218	-	-	-	-	-
[20]	Fatigue	F	1000	IPE120	208	330	444	NM	2.8	195	>2800	Sikadur 30 Sikadur 330	-	>4.5 >3.8	>28.4 >30	-
[22]	Fatigue	F	-	IPE120	199.3	383	462	NM HM UHM	1.4	159 220 440	2800 2800 1200	Araldite AW106	-	-	-	-
[24]	Fatigue	F	1000	IPE120	208	330	444	HM	1.4	205	3200	Sikadur 30 Sikadur 330	-	>4.5 >3.8	>28.4 >30	-
[17]	Static	T	3000	UB203 × 102 × 23	190	335	429	Hybrid CFRP-GFRP	3.175 6.35	62.19	852	-	-	-	[17]	-
[123]	Fatigue	F	-	I-shaped	192.8	378.2	519	NM	-	200.4	3022.4	-	-	-	[123]	-
[105]	Static	F	2000	H-section	185	210.4	332.1	NM	1.2	167.3	2398.3	Sikadur-30	-	11.3	22.3	-
[123]	Fatigue	F	-	I-shaped	192.8	378.2	519	HM	-	200.4	3022.4	Araldite 420 Sikadur 30	-	1.495 11.2	29 30	-
[27]	Fatigue	F	-	I-shaped	192.8	378.2	519	HM	-	200.4	3022.4	Araldite 420 Sikadur 30	-	1.495 11.2	29 30	-
[124]	Fatigue	F	1300	H-section	197.3	158.8	-	NM	2	183.2	2239.5	Lica-131	-	5.7	39.2	-

* Test setup: T = Three-point bending/F = Four-point bending; ** Steel/concrete composite beam.

As for the type of adhesives, it was found that adhesives with relatively high ductility can effectively redistribute stress within the adhesive layer during increased loading [121]. Consequently, it is suggested to use nonlinear adhesives for retrofitting steel structures as the specimens bonded with linear adhesives are more susceptible to interfacial debonding [123].

Prestressing CFRP sheets can effectively increase the fatigue life of cracked steel elements as compressive forces are applied to the crack edges, thereby hindering crack growth in steel structures [21]. It was also shown that the prestressed CFRP can decrease the interfacial stress at the notch location and delay interfacial debonding [124]. Also, the level of the prestressing of the CFRP has a significant effect on extending the fatigue life of strengthened specimens [120]. The minimum level for prestressing the CFRP needed to increase the fatigue life of steel beams was determined in the literature [125].

4. Numerical Analysis

Computational methods present a cost-effective tool for a better understanding of the performance of the retrofitted components. In this regard, many numerical studies have been proposed to investigate the bond behavior of the retrofitted elements with CFRP.

Peiris [39] investigated a numerical study on the bond behavior of CFRP/steel joints using ANSYS (2009) software for NM and UHM CFRP by analyzing double-strap joint and doubly reinforced steel plates. An eight-node element of SOLID45 was used due to its large deflection and strain capabilities. The CFRP layer and adhesive were modeled as a single layer of elements. The results showed that the numerical element strains are in good agreement with experimental results except at the gap of the joints. Furthermore, the tensile stress obtained from finite element (FE) analysis is less than the experimental ones for ultra-high modulus CFRP. In this study, steel beams strengthened with UHM CFRP were also modeled. Contrary to CFRP/steel joint models, 4-node SHELL181 elements were utilized to simulate beams to reduce the computational costs. However, the proposed model could not predict the failure of the beam or the laminate for strip panel configuration as a result of the simplified assumptions of the SHELL181 element.

Wu and Zhao [60] modeled CFRP/steel joints using ABAQUS software, utilizing CPE4R elements for the CFRP and steel adherents and COH2D4 elements for the adhesive layer. The tie constraint, used in ABAQUS to establish perfect interface connection, was applied to the CFRP/adhesive and steel/adhesive surfaces. The numerical findings aligned well with experimental results in terms of the ultimate load, and bond–slip relationships. Al-Mosawe et al. [46] presented a numerical investigation of the effect of high load rates on the bond behavior of CFRP/steel double strap joints using ABAQUS for LM and NM CFRP. The C3D8R, SC8R, and COH3D8 elements were utilized to model steel plates, CFRP laminate, and the adhesive layer, respectively. The tie constraint was also applied to the adhesive layer with steel and CFRP. It was found that the effective bond length for specimens subjected to high loading rates was shorter compared to the specimens tested under quasi-static loading.

The flexural behavior of steel beams strengthened with CFRP sheets using ANSYS was studied by Elkhabeery et al. [18]. SOLID186 elements were selected to model steel and CFRP sheets. To model the epoxy layer, the INTER204 element was used. The adhesive layer was defined as linear elastic material and the mixed-mode bi-linear cohesive zone model (CZM) was selected to model the bond between steel and CFRP. The parametric study showed that the CFRP system is very efficient in strengthening compact mono-symmetric sections, whereas its effect is very negligible for non-compact sections. The CFRP/steel double overlapped bonded joints were simulated by Yang et al. [77]. It was revealed that the initial stiffness of the load versus slip relationship increases with the elastic modulus of CFRP laminate. Colombi et al. [106] carried out a numerical study on the static behavior of the steel beams strengthened with CFRP strips. A standard two nodes beam element was applied to model the beam and a standard eight-node plane stress element was selected to model CFRP strips as well as the adhesive layer. To ensure the compatibility

of the deformations of the beams and strips, multipoint constraints were imposed between the beam nodes and the corresponding adhesive nodes. The adhesive stresses estimated by the FE model were in good agreement with their counterparts obtained from the analytical approach. A 2D FE model was proposed by Lenwari [122] to investigate the debonding strength of steel beams strengthened with CFRP. To this end, the eight-node element with two degrees of freedom at each node was utilized. Furthermore, it was assumed that the CFRP material is isotropic. The results indicated that the adhesive modulus, the CFRP thickness, and the CFRP modulus significantly affect the debonding strength. Fernando [59] studied the prediction of the debonding failure in RHS steel tubes strengthened with CFRP using a bond–slip model under an end-bearing load. C3D8, S4R, and COH3D8 elements were used to model the bearing plate, CFRP plate, and adhesive layer. The tie constraint was applied to adhesive surfaces connected to the CFRP plate and tub web. The results indicated that the debonding process in the FE model is much more gradual which can lead to higher stiffness in the load–displacement curve prior to reaching the ultimate load. A numerical investigation on the interfacial behavior of the bond between CFRP laminate and steel beam was presented by Linghoff et al. [126]. In this study, all parts were modeled using C3D20R solid elements and the common nodes at the interfaces were merged. It is found that interfacial shear stress as well as peel stress are not uniformly distributed over the width of the adhesive layer. Furthermore, the distribution of the peeling stresses along the width of the bond-line is not the same for different strengthened beams. This variation is attributed to the higher axial stiffness of the CFRP laminate as a major parameter. Hmidan et al. [16] investigated the flexural behavior of the steel beams repaired with CFRP sheets with various initial crack configurations by simulating a three-dimensional model in ANSYS. SOLID45 and LINK8 elements were utilized to model steel beams and CFRP sheets, respectively. These elements can be connected using interface elements as they have the same degree of freedom. The COMIN39 interface element was used to predefine crack propagation at the midspan of the beam. Results showed that the influence of the initial damage level on the failure mode of the repaired beam is negligible, whereas the damage level can have an effect on the web fracture rate of the beams. Moreover, the level of the initial damage determines the initiation of CFRP debonding. Deng [127] studied the rehabilitation of notched steel beams using CFRP plates. In this regard, a mixed-mode cohesive law was used to model notched retrofitted steel beams. The findings show that increasing the CFRP elastic modulus and thickness can enhance the bearing capacity while reducing the ductility and leading to premature debonding failure. Wang et al. [128] explored the effectiveness of using externally bonded CFRP using ductile adhesive. A trapezoidal mixed-mode CZM was used to simulate the debonding behavior of the CFRP-strengthened steel beam. The findings revealed that thicker or shorter CFRP laminates resulted in higher interfacial stresses, leading to earlier debonding, whereas longer CFRP laminates delayed debonding by changing the stress transfer path.

Table 7 provides a summary of the numerical studies presented in the literature. The realistic representation of stress distribution and failure modes in the rehabilitated elements with CFRP demands high computational costs. However, simplifications of the assumptions may not capture all real-world behaviors. Therefore, finding a middle ground that takes these factors into account is really important.

Table 7. Summary of numerical studies.

Study	Software	Steel Element Type	CFRP Element Type	Adhesive Element Type	Interactions
[39]	ANSYS (2009)	8-node SOLID45	8-node SOLID45	8-node SOLID45	Perfect interface
[60]	ABAQUS (V6.8)	CPE4R	CPE4R	COH2D4	Quadratic traction damage initiation criterion
[46]	ABAQUS (V6.13)	C3D8R	SC8R	COH3D8	Tie constraint
[18]	ANSYS (V17)	SOLID186	SOLID186	INTER204	Mixed-mode bi-linear CZM
[77]	ABAQUS	T2D2	T2D2	COH2D4	Bi-linear bond–slip derived from experimental data
[106]	ABAQUS	2-node beam element	8-node plane stress element	8-node plane stress element	Multipoint constraints
[122]	Not specified	8-node element with 2 DOF per node	8-node element with 2 DOF per node	Not specified	Reciprocal work contour integral method
[59]	ABAQUS (2004)	C3D8	S4R	COH3D8	Tie constraint
[126]	ABAQUS (V6.4.1)	C3D20R	C3D20R	C3D20R	Common nodes merged
[16]	ANSYS	SOLID45	LINK8	COMBIN39	Bi-linear bond–slip model
[127]	ABAQUS	C3D8I	COH3D8	COH3D8	Mixed-mode cohesive law
[128]	ABAQUS	C3D8I	C3D8R	COH3D8	Trapezoidal mixed-mode CZM

5. Research Needs and Recommendations

A review of all the investigations regarding the application of CFRP materials for the retrofitting of steel members suggests that research in this area is rather limited. The number of parameters affecting the behavior of CFRP retrofitted steel members increases the complexity of their behavior. Accordingly, many experimental programs are needed to investigate the effect of these parameters. Furthermore, there are limited numerical investigations that can accurately predict the behavior of CFRP retrofitted steel components. Hence, special attention needs to be devoted to developing reliable numerical modeling. Although the applied CFRP in the literature includes various elastic moduli, investigations involving UHM CFRP have not been adequately documented. Therefore, further research is needed in this regard. Further investigations on the behavior of steel components retrofitted with CFRP could be conducted in the following recommended research areas:

- Further investigation is needed to develop adhesives with enhanced mechanical properties to improve bond strength and durability.
- Further research should be conducted to investigate the effect of interrelated parameters on the bond behavior of the CFRP/steel interface to propose an optimal retrofitting system. The finite element modeling can be considered a cost-effective solution in this regard.
- To better analyze the impact of the CFRP elastic modulus on the performance of the retrofitted steel elements, it is advisable to use CFRPs with approximately the same tensile capacity but varying elastic modulus.
- More investigation is required to develop bond–slip models at the CFRP/steel interface under fatigue loading by considering the influencing variables that are representative of conditions in practice.
- More research is needed to investigate the effect of fatigue loading on the effective bond length. Also, the effect of shear combined with flexure on the bond length is to be clarified.
- More research could be conducted to investigate the effect of galvanic corrosion, especially in the CFRP retrofitting method utilizing a steel anchorage system. The long-term effect of galvanic corrosion has not been properly investigated.

6. Conclusions

A state of knowledge on the application of the CFRP in retrofitting steel elements as well as the influencing parameters is presented. Based on the findings obtained from the available literature, the following conclusions can be drawn:

- Using CFRP with higher elastic modulus results in an increase in CFRP/steel bond strength and contributes to an improvement of the performance of retrofitted steel components by increasing structural load-carrying capacity and flexural strength.

- Applying adhesives with higher tensile modulus generally results in enhanced bond strength of the steel/CFRP interface. Nevertheless, adhesives with nonlinear properties can yield higher failure loads than linear adhesives with an even higher tensile modulus.

- As for bond–slip models, studies have shown that in linear adhesive materials, triangular bond–slip curves are obtained, whereas in nonlinear adhesives, the bond–slip relationship tends to follow a trapezoidal curve.

- Proper surface preparation of steel substrates is crucial for achieving a strong bond strength. Mechanical treatments like grit blasting improve surface roughness and chemical bonding.

- Increasing the elastic modulus of CFRP reinforcement could lead to an improvement in the fatigue life of specimens. Indeed, it has been found that the fatigue life of a steel structure can be enhanced by either applying prestressing to the steel details or by increasing beam stiffness by using UHM CFRP or adding CFRP layers.

- Regarding the performance of prestressed CFRP, experimental results indicate that prestressing can reduce the stress intensity factor and confine crack growth by applying compressive forces to the edges of cracks in notched steel elements. Therefore, the use of prestressed CFRP patches could enhance the effectiveness of CFRP rehabilitation systems.

- Finally, experimental studies of anchorage systems have shown that using anchorage techniques can help delay crack propagation and thereby prolong fatigue life in strengthened steel specimens. The crack mouth opening displacement could also be reduced as a result of using anchorage systems.

Data Availability Statement: Not applicable.

Conflicts of Interest: The authors declare no conflict of interest.

Notations

b_p	Width of CFRP plate
b_s	Width of steel plate
E_a	Young's modulus of adhesive
E_p	Young's modulus of CFRP plate
E_s	Young's modulus of steel plate
h_b	Height of beam
f_a	Tensile strength of adhesive
f_p	CFRP tensile strength
f_y	Steel yield stress
f_u	Steel ultimate stress
G_a	Shear modulus of adhesive
G_f	Interfacial fracture energy
L_e	Effective bond length of CFRP plate
$L_{span,b}$	Span length of steel beam
N	Number of interfaces working in parallel
P_u	Ultimate load (bond strength)
t_a	Thickness of adhesive layer

t_p	Thickness of CFRP plate
t_s	Thickness of steel plate
W_b	Width of beam
W_s	Steel plate width
τ_f	Peak interfacial shear stress
τ^*	Interlaminar shear strength of the CFRP plate
δ_1	Relative slip corresponding to the peak interfacial stress
δ_2	Relative slip when the shear stress begins to decrease in the tri-linear model
δ_f	Maximum slip

References

1. Dexter, R.J.; Ocel, J.M. *Manual for Repair and Retrofit of Fatigue Cracks in Steel Bridges*; Federal Highway Administration: Ashburn, VA, USA, 2013.
2. Schnerch, D.; Dawood, M.; Rizkalla, S.; Sumner, E. Proposed design guidelines for strengthing of steel bridges with FRP materials. *Constr. Build. Mater.* **2007**, *21*, 1001–1010. [CrossRef]
3. Fisher, J.W. Evolution of fatigue-resistant steel bridges. *Transp. Res. Rec. J. Transp. Res. Board* **1997**, *1594*, 5–17. [CrossRef]
4. Tavakkolizadeh, M.; Saadatmanesh, H. Fatigue strength of steel girders strengthened with carbon fiber reinforced polymer patch. *J. Struct. Eng.* **2003**, *129*, 186–196. [CrossRef]
5. Zhao, X.-L.; Zhang, L. State-of-the-art review on FRP strengthened steel structures. *Eng. Struct.* **2007**, *29*, 1808–1823. [CrossRef]
6. Hollaway, L.C.; Cadei, J. Progress in the technique of upgrading metallic structures with advanced polymer composites. *Prog. Struct. Eng. Mater.* **2002**, *4*, 131–148. [CrossRef]
7. Kamruzzaman, M.; Jumaat, M.Z.; Sulong, N.H.R.; Islam, A.B.M.S. A review on strengthening steel beams using FRP under fatigue. *Sci. World J.* **2014**, *2014*, 702537. [CrossRef] [PubMed]
8. Oudah, F.; El-Hacha, R. Research progress on the fatigue performance of RC beams strengthened in flexure using Fiber Reinforced Polymers. *Compos. Part B Eng.* **2013**, *47*, 82–95. [CrossRef]
9. Chataigner, S.; Benzarti, K.; Foret, G.; Caron, J.; Gemignani, G.; Brugiolo, M.; Calderon, I.; Piñero, I.; Birtel, V.; Lehmann, F. Design and testing of an adhesively bonded CFRP strengthening system for steel structures. *Eng. Struct.* **2018**, *177*, 556–565. [CrossRef]
10. Hu, B.; Li, Y.; Jiang, Y.-T.; Tang, H.-Z. Bond behavior of hybrid FRP-to-steel joints. *Compos. Struct.* **2020**, *237*, 111936. [CrossRef]
11. Jagtap, P.; Pore, S.; Prakash, V. Necessity of strengthening of steel structures with FRP composites: A review. *Int. J. Latest Trends Eng. Technol. (IJLTET)* **2015**, *5*, 390–394.
12. Shaat, A.; Fam, A. Repair of cracked steel girders connected to concrete slabs using carbon-fiber-reinforced polymer sheets. *J. Compos. Constr.* **2008**, *12*, 650–659. [CrossRef]
13. Schnerch, D.; Rizkalla, S. Flexural strengthening of steel bridges with high modulus CFRP strips. *J. Bridg. Eng.* **2008**, *13*, 192–201. [CrossRef]
14. Fam, A.; MacDougall, C.; Shaat, A. Upgrading steel–concrete composite girders and repair of damaged steel beams using bonded CFRP laminates. *Thin-Walled Struct.* **2009**, *47*, 1122–1135. [CrossRef]
15. Linghoff, D.; Al-Emrani, M.; Kliger, R. Performance of steel beams strengthened with CFRP laminate—Part 1: Laboratory tests. *Compos. Part B Eng.* **2010**, *41*, 509–515. [CrossRef]
16. Hmidan, A.; Kim, Y.J.; Yazdani, S. CFRP Repair of Steel Beams with Various Initial Crack Configurations. *J. Compos. Constr.* **2011**, *15*, 952–962. [CrossRef]
17. Sweedan, A.M.; Alhadid, M.M.; El-Sawy, K.M. Experimental study of the flexural response of steel beams strengthened with anchored hybrid composites. *Thin-Walled Struct.* **2016**, *99*, 1–11. [CrossRef]
18. Elkhabeery, O.H.; Safar, S.S.; Mourad, S.A. Flexural strength of steel I-beams reinforced with CFRP sheets at tension flange. *J. Constr. Steel Res.* **2018**, *148*, 572–588. [CrossRef]
19. Wu, C.; Zhao, X.L.; Chiu, W.K.; Al-Mahaidi, R.; Duan, W.H. Effect of fatigue loading on the bond behaviour between UHM CFRP plates and steel plates. *Compos. Part B Eng.* **2013**, *50*, 344–353. [CrossRef]
20. Colombi, P.; Fava, G. Experimental study on the fatigue behaviour of cracked steel beams repaired with CFRP plates. *Eng. Fract. Mech.* **2015**, *145*, 128–142. [CrossRef]
21. Emdad, R.; Al-Mahaidi, R. Effect of prestressed CFRP patches on crack growth of centre-notched steel plates. *Compos. Struct.* **2015**, *123*, 109–122. [CrossRef]
22. Ghafoori, E. Fatigue Strengthening of Metallic Members Using Un-Bonded and Bonded CFRP Laminates. Ph.D. Thesis, ETH Zurich, Zurich, Switzerland, 2015.
23. Aljabar, N.; Zhao, X.; Al-Mahaidi, R.; Ghafoori, E.; Motavalli, M.; Powers, N. Effect of crack orientation on fatigue behavior of CFRP-strengthened steel plates. *Compos. Struct.* **2016**, *152*, 295–305. [CrossRef]
24. Colombi, P.; Fava, G. Fatigue crack growth in steel beams strengthened by CFRP strips. *Theor. Appl. Fract. Mech.* **2016**, *85*, 173–182. [CrossRef]
25. Hu, L.L.; Zhao, X.L.; Feng, P. Fatigue Behavior of Cracked High-Strength Steel Plates Strengthened by CFRP Sheets. *J. Compos. Constr.* **2016**, *20*, 04016043. [CrossRef]

26. Aljabar, N.; Zhao, X.; Al-Mahaidi, R.; Ghafoori, E.; Motavalli, M.; Koay, Y. Fatigue tests on UHM-CFRP strengthened steel plates with central inclined cracks under different damage levels. *Compos. Struct.* **2017**, *160*, 995–1006. [CrossRef]

27. Yu, Q.-Q.; Wu, Y.-F. Fatigue retrofitting of cracked steel beams with CFRP laminates. *Compos. Struct.* **2018**, *192*, 232–244. [CrossRef]

28. Tafsirojjaman, T.; Fawzia, S.; Thambiratnam, D.P.; Zhao, X.-L. FRP strengthened SHS beam-column connection under monotonic and large-deformation cyclic loading. *Thin-Walled Struct.* **2021**, *161*, 107518. [CrossRef]

29. Tong, L.; Xu, G.; Zhao, X.-L.; Yan, Y. Fatigue tests and design of CFRP-strengthened CHS gap K-joints. *Thin-Walled Struct.* **2021**, *163*, 107694. [CrossRef]

30. Wang, H.-T.; Wu, G.; Pang, Y.-Y.; Shi, J.-W.; Zakari, H.M. Experimental study on the bond behavior between CFRP plates and steel substrates under fatigue loading. *Compos. Part B Eng.* **2019**, *176*, 107266. [CrossRef]

31. Ke, L.; Li, C.; He, J.; Shen, Q.; Liu, Y.; Jiao, Y. Enhancing fatigue performance of damaged metallic structures by bonded CFRP patches considering temperature effects. *Mater. Des.* **2020**, *192*, 108731. [CrossRef]

32. Liu, X. *Rehabilitation of Steel Bridge Members with FRP Composite Materials*; University of Missouri-Rolla: Rolla, MO, USA, 2003.

33. Ghafoori, E.; Motavalli, M. Normal, high and ultra-high modulus carbon fiber-reinforced polymer laminates for bonded and un-bonded strengthening of steel beams. *Mater. Des.* **2015**, *67*, 232–243. [CrossRef]

34. Yu, T.; Fernando, D.; Teng, J.; Zhao, X. Experimental study on CFRP-to-steel bonded interfaces. *Compos. Part B Eng.* **2012**, *43*, 2279–2289. [CrossRef]

35. Stanford, K.A. Strengthening of Steel Structures with High Modulus Carbon Fiber Reinforced Polymers (CRRP) Materials: Bond and Development Length Study. Master's Thesis, North Carolina State University, Raleigh, NC, USA, 2009.

36. Gholami, M.; Sam, A.R.M.; Yatim, J.M.; Tahir, M.M. A review on steel/CFRP strengthening systems focusing environmental performance. *Constr. Build. Mater.* **2013**, *47*, 301–310. [CrossRef]

37. Borrie, D.; Al-Saadi, S.; Zhao, X.-L.; Raman, R.K.S.; Bai, Y. Bonded CFRP/Steel Systems, Remedies of Bond Degradation and Behaviour of CFRP Repaired Steel: An Overview. *Polymers* **2021**, *13*, 1533. [CrossRef]

38. Duncan, B. Developments in testing adhesive joints. In *Advances in Structural Adhesive Bonding*; Elsevier: Amsterdam, The Netherlands, 2010; pp. 389–436.

39. Peiris, N.A. *Steel Beams Strengthened with Ultra High Modulus CFRP Laminates*; University of Kentucky: Lexington, KY, USA, 2011.

40. Jiao, H.; Zhao, X.-L. CFRP strengthened butt-welded very high strength (VHS) circular steel tubes. *Thin-Walled Struct.* **2004**, *42*, 963–978. [CrossRef]

41. Fawzia, S.; Zhao, X.; Al-Mahaidi, R.; Rizkalla, S. Bond characteristics between CFRP and steel plates in double strap joints. *Adv. Steel Constr.* **2005**, *1*, 17–27.

42. He, J.; Xian, G.; Zhang, Y. Effect of moderately elevated temperatures on bond behaviour of CFRP-to-steel bonded joints using different adhesives. *Constr. Build. Mater.* **2020**, *241*, 118057. [CrossRef]

43. Zhou, H.; Fernando, D.; Torero, J.L.; Torres, J.P.; Maluk, C.; Emberley, R. Bond Behavior of CFRP-to-Steel Bonded Joints at Mild Temperatures: Experimental Study. *J. Compos. Constr.* **2020**, *24*, 04020070. [CrossRef]

44. Guo, X.; Wu, Z.; Yang, Y.; Bai, J.; Zhou, Q. A Study on the Bond–Slip Relationship of the CFRP–Steel Interface of CFRP Strengthened Steel. *Materials* **2022**, *15*, 4187. [CrossRef]

45. Li, Y.; Li, C.; He, J.; Gao, Y.; Hu, Z. Effect of functionalized nano-SiO_2 addition on bond behavior of adhesively bonded CFRP-steel double-lap joint. *Constr. Build. Mater.* **2020**, *244*, 118400. [CrossRef]

46. Al-Mosawe, A.; Al-Mahaidi, R.; Zhao, X.-L. Bond behaviour between CFRP laminates and steel members under different loading rates. *Compos. Struct.* **2016**, *148*, 236–251. [CrossRef]

47. He, J.; Xian, G. Debonding of CFRP-to-steel joints with CFRP delamination. *Compos. Struct.* **2016**, *153*, 12–20. [CrossRef]

48. Al-Mosawe, A.; Al-Mahaidi, R. Performance of CFRP-steel joints enhanced with bi-directional CFRP fabric. *Constr. Build. Mater.* **2019**, *197*, 72–82. [CrossRef]

49. Wang, H.-T.; Wu, G. Bond-slip models for CFRP plates externally bonded to steel substrates. *Compos. Struct.* **2018**, *184*, 1204–1214. [CrossRef]

50. Li, C.; Ke, L.; He, J.; Chen, Z.; Jiao, Y. Effects of mechanical properties of adhesive and CFRP on the bond behavior in CFRP-strengthened steel structures. *Compos. Struct.* **2019**, *211*, 163–174. [CrossRef]

51. Zhou, H.; Liu, H.Y.; Zhou, H.; Zhang, Y.; Gao, X.; Mai, Y.W. On adhesive properties of nano-silica/epoxy bonded single-lap joints. *Mater. Des.* **2016**, *95*, 212–218. [CrossRef]

52. Sousa, J.M.; Correia, J.R.; Cabral-Fonseca, S. Durability of an epoxy adhesive used in civil structural applications. *Constr. Build. Mater.* **2018**, *161*, 618–633. [CrossRef]

53. Ferreira, F.V.; Brito, F.S.; Franceschi, W.; Simonetti, E.A.N.; Cividanes, L.S.; Chipara, M.; Lozano, K. Functionalized graphene oxide as reinforcement in epoxy based nanocomposites. *Surf. Interfac.* **2018**, *10*, 100–109. [CrossRef]

54. Wan, Y.-J.; Gong, L.-X.; Tang, L.-C.; Wu, L.-B.; Jiang, J.-X. Mechanical properties of epoxy composites filled with silane-functionalized graphene oxide. *Compos. Part A Appl. Sci. Manuf.* **2014**, *64*, 79–89. [CrossRef]

55. Xie, G.-H.; You, Y.; Tao, Z.-A.; Li, S.-Q. Experimental and theoretical study on mechanical behaviors of CFRP-steel interface. *Thin-Walled Struct.* **2023**, *182*, 110208. [CrossRef]

56. Razavi, N.; Ayatollahi, M.R.; Giv, A.N.; Khoramishad, H. Single lap joints bonded with structural adhesives reinforced with a mixture of silica nanoparticles and multi walled carbon nanotubes. *Int. J. Adhes. Adhes.* **2018**, *80*, 76–86. [CrossRef]

57. Saraç, I.; Adin, H.; Temiz, Ş. Experimental determination of the static and fatigue strength of the adhesive joints bonded by epoxy adhesive including different particles. *Compos. Part B Eng.* **2018**, *155*, 92–103. [CrossRef]

58. Mohabeddine, A.; Malik, G.; Correia, J.; Silva, F.; De Jesus, A.; Fantuzzi, N.; Castro, J.M. Experimental parametric investigation on the behavior of adhesively bonded CFRP/steel joints. *Compos. Struct.* **2023**, *307*, 116598. [CrossRef]

59. Fernando, N.D. Bond Behaviour and Debonding Failures in CFRP-Strengthened Steel Members. Ph.D. Thesis, The Hong Kong Polytechnic University, Hong Kong, China, 2010.

60. Wu, C.; Zhao, X.; Duan, W.H.; Al-Mahaidi, R. Bond characteristics between ultra high modulus CFRP laminates and steel. *Thin-Walled Struct.* **2012**, *51*, 147–157. [CrossRef]

61. Wang, H.-T.; Wu, G.; Dai, Y.-T.; He, X.-Y. Experimental Study on Bond Behavior between CFRP Plates and Steel Substrates Using Digital Image Correlation. *J. Compos. Constr.* **2016**, *20*, 04016054. [CrossRef]

62. Wang, H.-T.; Wu, G.; Dai, Y.-T.; He, X.-Y. Determination of the bond–slip behavior of CFRP-to-steel bonded interfaces using digital image correlation. *J. Reinf. Plast. Compos.* **2016**, *35*, 1353–1367. [CrossRef]

63. Xia, S.; Teng, J. Behaviour of FRP-to-steel bonded joints. In *International Symposium on Bond Behaviour of FRP in Structures, BBFS 2005*; International Institute for FRP in Construction (IIFC): Hong Kong, China, 2005.

64. Photiou, N.K. *Rehabilitation of Steel Members Utilising Hybrid FRP Composite Material Systems*; University of Surrey (United Kingdom): Guildford, UK, 2005.

65. Fawzia, S. Bond Characteristics between Steel and Carbon Fibre Reinforced Polymer (CFRP) Composites. Ph.D. Thesis, Monash University, Clayton, Australia, 2007.

66. The Institution of Structural Engineers (ISE). *The Structural Use of Adhesives*; The Institution of Structural Engineers (ISE): London, UK, 1999.

67. Fawzia, S.; Zhao, X.-L.; Al-Mahaidi, R. Bond–slip models for double strap joints strengthened by CFRP. *Compos. Struct.* **2010**, *92*, 2137–2145. [CrossRef]

68. Heshmati, M.; Haghani, R.; Al-Emrani, M.; André, A. On the strength prediction of adhesively bonded FRP-steel joints using cohesive zone modelling. *Theor. Appl. Fract. Mech.* **2018**, *93*, 64–78. [CrossRef]

69. Fawzia, S. Evaluation of shear stress and slip relationship of composite lap joints. *Compos. Struct.* **2013**, *100*, 548–553. [CrossRef]

70. Wu, C.; Yu, Y.-Z.; Tam, L.-H.; Orr, J.; He, L. Effect of glass fiber sheet in adhesive on the bond and galvanic corrosion behaviours of CFRP-Steel bonded system. *Compos. Struct.* **2021**, *259*, 113218. [CrossRef]

71. Wu, C.; Yu, Y.-Z.; Tam, L.-H.; He, L. Effects of bondline defects on the bond behaviour of CFRP-steel double strap joints. *Compos. Struct.* **2023**, *308*, 116682. [CrossRef]

72. Schnerch, D.; Dawood, M.; Rizkalla, S.; Sumner, E.; Stanford, K. Bond behavior of CFRP strengthened steel structures. *Adv. Struct. Eng.* **2006**, *9*, 805–817. [CrossRef]

73. Colombi, P.; Poggi, C. Strengthening of tensile steel members and bolted joints using adhesively bonded CFRP plates. *Constr. Build. Mater.* **2006**, *20*, 22–33. [CrossRef]

74. Nguyen, T.-C.; Bai, Y.; Zhao, X.-L.; Al-Mahaidi, R. Curing effects on steel/CFRP double strap joints under combined mechanical load, temperature and humidity. *Constr. Build. Mater.* **2013**, *40*, 899–907. [CrossRef]

75. He, J.; Xian, G. Bond-slip behavior of fiber reinforced polymer strips-steel interface. *Constr. Build. Mater.* **2017**, *155*, 250–258. [CrossRef]

76. Peiris, A.; Harik, I. FRP-steel bond study of IM and UHM CFRP strips. *Constr. Build. Mater.* **2018**, *185*, 628–637. [CrossRef]

77. Yang, Y.; Zhao, J.; Zhang, S.; Chastre, C.; Biscaia, H. Effect of mechanical anchorage on the bond performance of double overlapped CFRP-to-steel joints. *Compos. Struct.* **2021**, *267*, 113902. [CrossRef]

78. Fernando, D.; Teng, J.G.; Yu, T.; Zhao, X.L. Preparation and characterization of steel surfaces for adhesive bonding. *J. Compos. Constr.* **2013**, *17*, 04013012. [CrossRef]

79. Schnerch, D.A. Strengthening of Steel Structures with High Modulus Carbon Fiber Reinforced Polymer (CFRP) Materials. Ph.D. Thesis, North Carolina State University, Raleigh, NC, USA, 2005.

80. Lorenzo, M.A. Experimental Methods for Evaluating Epoxy Coating Adhesion to Steel Reinforcement. Master's Thesis, University of Texas at Austin, Austin, TX, USA, 1997.

81. Baldan, A. Adhesively-bonded joints and repairs in metallic alloys, polymers and composite materials: Adhesives, adhesion theories and surface pretreatment. *J. Mater. Sci.* **2004**, *39*, 1–49. [CrossRef]

82. Ebnesajjad, S.; Ebnesajjad, C. *Surface Treatment of Materials for Adhesive Bonding*; William Andrew: Norwich, NY, USA, 2013.

83. Ebnesajjad, S.; Landrock, A.H. *Adhesives Technology Handbook*, 2nd ed.; William Andrew: New York, NY, USA, 2014.

84. Islam, M.; Tong, L.; Falzon, P. Influence of metal surface preparation on its surface profile, contact angle, surface energy and adhesion with glass fibre prepreg. *Int. J. Adhes. Adhes.* **2014**, *51*, 32–41. [CrossRef]

85. Narmashiri, K.; Jumaat, M.Z.; Sulong, N.H.R. Strengthening of steel I-beams using CFRP strips: An investigation on CFRP bond length. *Adv. Struct. Eng.* **2012**, *15*, 2191–2204. [CrossRef]

86. Yang, Y.; Biscaia, H.; Chastre, C.; Silva, M.A. Bond characteristics of CFRP-to-steel joints. *J. Constr. Steel Res.* **2017**, *138*, 401–419. [CrossRef]

87. Fawzia, S.; Al-Mahaidi, R.; Zhao, X.-L. Experimental and finite element analysis of a double strap joint between steel plates and normal modulus CFRP. *Compos. Struct.* **2006**, *75*, 156–162. [CrossRef]

88. Bocciarelli, M.; Colombi, P.; Fava, G.; Poggi, C. Prediction of debonding strength of tensile steel/CFRP joints using fracture mechanics and stress based criteria. *Eng. Fract. Mech.* **2009**, *76*, 299–313. [CrossRef]

89. Chiew, S.; Yu, Y.; Lee, C. Bond failure of steel beams strengthened with FRP laminates—Part 1: Model development. *Compos. Part B Eng.* **2011**, *42*, 1114–1121. [CrossRef]

90. Al-Zubaidy, H.; Al-Mahaidi, R.; Zhao, X.-L. Experimental investigation of bond characteristics between CFRP fabrics and steel plate joints under impact tensile loads. *Compos. Struct.* **2012**, *94*, 510–518. [CrossRef]

91. Al-Zubaidy, H.; Al-Mahaidi, R.; Zhao, X.-L. Finite element modelling of CFRP/steel double strap joints subjected to dynamic tensile loadings. *Compos. Struct.* **2013**, *99*, 48–61. [CrossRef]

92. Korayem, A.H.; Li, C.Y.; Zhang, Q.H.; Zhao, X.L.; Duan, W.H. Effect of carbon nanotube modified epoxy adhesive on CFRP-to-steel interface. *Compos. Part B Eng.* **2015**, *79*, 95–104. [CrossRef]

93. Al-Zubaidy, H.A.; Zhao, X.-L.; Al-Mahaidi, R. Dynamic bond strength between CFRP sheet and steel. *Compos. Struct.* **2012**, *94*, 3258–3270. [CrossRef]

94. Huo, J.; Zhang, X.; Yang, J.; Xiao, Y. Experimental study on dynamic behavior of CFRP-to-steel interface. *Structures* **2019**, *20*, 465–475. [CrossRef]

95. Al-Zubaidy, H.A.; Zhao, X.-L.; Al-Mahaidi, R. Experimental evaluation of the dynamic bond strength between CFRP sheets and steel under direct tensile loads. *Int. J. Adhes. Adhes.* **2013**, *40*, 89–102. [CrossRef]

96. Chen, J.F.; Teng, J.G. Anchorage strength models for FRP and steel plates bonded to concrete. *J. Struct. Eng.* **2001**, *127*, 784–791. [CrossRef]

97. Bocciarelli, M.; Colombi, P.; Fava, G.; Poggi, C. Interaction of interface delamination and plasticity in tensile steel members reinforced by CFRP plates. *Int. J. Fract.* **2007**, *146*, 79–92. [CrossRef]

98. Dehghani, E.; Daneshjoo, F.; Aghakouchak, A.; Khaji, N. A new bond-slip model for adhesive in CFRP–steel composite systems. *Eng. Struct.* **2012**, *34*, 447–454. [CrossRef]

99. Fernando, D.; Yu, T.; Teng, J.G. Behavior of CFRP Laminates Bonded to a Steel Substrate Using a Ductile Adhesive. *J. Compos. Constr.* **2014**, *18*, 04013040. [CrossRef]

100. Monti, G.; Renzelli, M.; Luciani, P. FRP adhesion in uncracked and cracked concrete zones. In *Fibre-Reinforced Polymer Reinforcement for Concrete Structures: (In 2 Volumes)*; World Scientific: Singapore, 2003; pp. 183–192.

101. Lu, X.Z.; Teng, J.G.; Ye, L.P.; Jiang, J.J. Bond–slip models for FRP sheets/plates bonded to concrete. *Eng. Struct.* **2005**, *27*, 920–937. [CrossRef]

102. Pang, Y.-Y.; Wu, G.; Wang, H.-T.; Su, Z.-L.; He, X.-Y. Experimental study on the bond behavior of the CFRP-steel interface under the freeze–thaw cycles. *J. Compos. Mater.* **2019**, *54*, 13–29. [CrossRef]

103. Wang, H.-T.; Liu, S.-S.; Liu, Q.-L.; Pang, Y.-Y.; Shi, J.-W. Influences of the joint and epoxy adhesive type on the CFRP-steel interfacial behavior. *J. Build. Eng.* **2021**, *43*, 103167. [CrossRef]

104. Pang, Y.; Wu, G.; Wang, H.; Gao, D.; Zhang, P. Bond-slip model of the CFRP-steel interface with the CFRP delamination failure. *Compos. Struct.* **2021**, *256*, 113015. [CrossRef]

105. Zeng, J.-J.; Gao, W.-Y.; Liu, F. Interfacial behavior and debonding failures of full-scale CFRP-strengthened H-section steel beams. *Compos. Struct.* **2018**, *201*, 540–552. [CrossRef]

106. Colombi, P.; Poggi, C. An experimental, analytical and numerical study of the static behavior of steel beams reinforced by pultruded CFRP strips. *Compos. Part B Eng.* **2006**, *37*, 64–73. [CrossRef]

107. Sallam, H.E.M.; Ahmad, S.S.E.; Badawy, A.A.M.; Mamdouh, W. Evaluation of steel I-Beams strengthened by various plating methods. *Adv. Struct. Eng.* **2006**, *9*, 535–544. [CrossRef]

108. Deng, J.; Lee, M.M. Behaviour under static loading of metallic beams reinforced with a bonded CFRP plate. *Compos. Struct.* **2007**, *78*, 232–242. [CrossRef]

109. Teng, J.; Fernando, D.; Yu, T. Finite element modelling of debonding failures in steel beams flexurally strengthened with CFRP laminates. *Eng. Struct.* **2015**, *86*, 213–224. [CrossRef]

110. Peiris, A.; Harik, I. Steel beam strengthening with UHM CFRP strip panels. *Eng. Struct.* **2021**, *226*, 111395. [CrossRef]

111. Teng, J.; Yu, T.; Fernando, D. Strengthening of steel structures with fiber-reinforced polymer composites. *J. Constr. Steel Res.* **2012**, *78*, 131–143. [CrossRef]

112. Al-Saidy, A.H. *Structural Behavior of Composite Steel Beams Strengthened/Repaired with Carbon Fiber Reinforced Polymer Plates*; Iowa State University: Ames, IA, USA, 2001.

113. Tabrizi, S.; Kazem, H.; Rizkalla, S.; Kobayashi, A. New small-diameter CFRP material for flexural strengthening of steel bridge girders. *Constr. Build. Mater.* **2015**, *95*, 748–756. [CrossRef]

114. Narmashiri, K.; Sulong, N.R.; Jumaat, M.Z. Failure analysis and structural behaviour of CFRP strengthened steel I-beams. *Constr. Build. Mater.* **2012**, *30*, 1–9. [CrossRef]

115. Karam, E.C. Retrofitting of Composite Steel Beams Pre-Damaged in Flexure using Fiber Reinforced Polymers. Master's Thesis, American University of Sharjah, Sharjah, United Arab Emirates, 2015.

116. Wang, H.-T.; Bian, Z.-N.; Chen, M.-S.; Hu, L.; Wu, Q. Flexural strengthening of damaged steel beams with prestressed CFRP plates using a novel prestressing system. *Eng. Struct.* **2023**, *284*, 115953. [CrossRef]

117. Yu, Q.-Q.; Wu, Y.-F. Fatigue durability of cracked steel beams retrofitted with high-strength materials. *Constr. Build. Mater.* **2017**, *155*, 1188–1197. [CrossRef]

118. Wu, G.; Wang, H.-T.; Wu, Z.-S.; Liu, H.-Y.; Ren, Y. Experimental study on the fatigue behavior of steel beams strengthened with different fiber-reinforced composite plates. *J. Compos. Constr.* **2012**, *16*, 127–137. [CrossRef]

119. Dawood, M.; Rizkalla, S.; Sumner, E. Fatigue and overloading behavior of steel–concrete composite flexural members strengthened with high modulus CFRP materials. *J. Compos. Constr.* **2007**, *11*, 659–669. [CrossRef]

120. Vatandoost, F. Fatigue Behaviour of Steel Girders Strengthened with Prestressed CFRP Strips. Master's Thesis, University of Waterloo, Waterloo, ON, Canada, 2010.

121. Nozaka, K.; Shield, C.K.; Hajjar, J.F. Effective bond length of carbon-fiber-reinforced polymer strips bonded to fatigued steel bridge I-girders. *J. Bridg. Eng.* **2005**, *10*, 195–205. [CrossRef]

122. Lenwari, A.; Thepchatri, T.; Albrecht, P. Debonding strength of steel beams strengthened with CFRP plates. *J. Compos. Constr.* **2006**, *10*, 69–78. [CrossRef]

123. Yu, Q.-Q.; Wu, Y.-F. Fatigue behaviour of cracked steel beams retrofitted with carbon fibre–reinforced polymer laminates. *Adv. Struct. Eng.* **2017**, *21*, 1148–1161. [CrossRef]

124. Li, J.; Zhu, M.; Deng, J. Flexural behaviour of notched steel beams strengthened with a prestressed CFRP plate subjected to fatigue damage and wetting/drying cycles. *Eng. Struct.* **2022**, *250*, 113430. [CrossRef]

125. Ghafoori, E.; Motavalli, M.; Nussbaumer, A.; Herwig, A.; Prinz, G.; Fontana, M. Determination of minimum CFRP pre-stress levels for fatigue crack prevention in retrofitted metallic beams. *Eng. Struct.* **2015**, *84*, 29–41. [CrossRef]

126. Linghoff, D.; Al-Emrani, M. Performance of steel beams strengthened with CFRP laminate—Part 2: FE analyses. *Compos. Part B Eng.* **2010**, *41*, 516–522. [CrossRef]

127. Deng, J.; Li, J.; Wang, Y.; Xie, W. Numerical study on notched steel beams strengthened by CFRP plates. *Constr. Build. Mater.* **2018**, *163*, 622–633. [CrossRef]

128. Wang, Z.; Xian, G.; Yue, Q. Finite element modeling of debonding failure in CFRP-strengthened steel beam using a ductile adhesive. *Compos. Struct.* **2023**, *311*, 116818. [CrossRef]